Wood Sci Technol (2016) 50:941–951
DOI 10.1007/s00226-016-0839-8

ORIGINAL

Effect of the desorption rate on the dimensional changes of *Eucalyptus saligna* wood

Leandro Passarini[1] · **Roger E. Hernández**[1]

Received: 9 October 2015 / Published online: 14 May 2016

Abstract Understanding the fundamental process involved in wood sorption and wood dimensional changes is essential to improve drying and to obtain high-quality end products at a reasonable price. The main objective of this study was to examine the dimensional behaviour and the wood–water relationships of never-dried *Eucalyptus saligna* wood under a wide range of moisture contents below and above the fibre saturation point (FSP). Four desorption conditions from full saturated state were carried out at 21 °C in several steps until 58 % relative humidity (RH) was reached. Slower desorption rates produced higher radial, tangential, and volumetric shrinkages. The estimated collapse was also higher for milder desorption rates, being greater in the tangential direction. However, desorption rates did not change the slope of shrinkage–equilibrium moisture content (EMC) curves in the 0–58 % RH range. Further, the FSP established by extending the straight linear portion of these curves to 0 % shrinkage revealed to be not reliable for a collapse-prone species like *E. saligna*. Finally, shrinkage–EMC curves suggest the presence of entrapped liquid water at RH higher than about 76 %, confirming the occurrence of a region in the hygroscopic range in which the loss of bound water takes place before all liquid water has been drained.

Introduction

Wood is a renewable and versatile material used for engineering and energy purposes. One of its main features is its high hygroscopicity, which allows wood to exchange water molecules with the surrounding environment until reaching a

✉ Roger E. Hernández
roger.hernandez@sbf.ulaval.ca

[1] Département Des Sciences du Bois et de la Forêt, Centre de Recherche sur les Matériaux Renouvelables, Université Laval, 2425, rue de la Terrasse, Quebec, QC G1V 0A6, Canada

dynamic equilibrium state, known as equilibrium moisture content (EMC) (Panshin and de Zeeuw 1980; Skaar 1988). Relative humidity (RH) plays an important role in EMC of wood, but other factors as temperature, sorption state (adsorption or desorption), mechanical stress, species, density, and extractable compounds may also be implied (Siau 1984). The concept of fibre saturation point (FSP) was introduced by Tiemann (1906) as the moisture content at which the cell walls are saturated with bound water, while the lumens are free of liquid water. This means that the FSP is a transition point between bound and liquid water (Stamm 1971). Below FSP, wood dimensional changes take place as a result of the loss and gain of moisture in the cell walls, being shrinkage and swelling consequences of internal deformations of the woody tissue (Panshin and de Zeeuw 1980; Forest Products Laboratory (FPL) 2010).

According to Shmulsky and Jones (2011), the variations in dimensions of a same species under the same RH are explained by the dimensions and size of the specimen, the wood density, and also drying rate. Except under steady conditions, drying rate assessment is technically demanding owing to the interaction between diffusion and capillary forces, both of which vary with environmental factors (Brown et al. 1952).

Eucalyptus is the most cultivated hardwood species in the world. The high growth rate, high adaptability to different soils and climates, ease of management by coppice, and valuable wood and non-wood products contribute to this success (Turnbull 1999). However, *Eucalyptus* wood has some problems, such as those associated with growth stresses, high shrinkage during drying, interlocked grain, and collapse, representing a challenge for the wood industry (FAO 1981). Its low permeability implies slow drying and development of high moisture gradients in boards. Consequently, drying becomes difficult and vulnerable to defects, mainly on backsawn boards (Vermaas 1995; Jankowsky and Santos 2005; Jankowsky et al. 2008). Control of drying becomes increasingly important as the supply of plantation timber rises, mainly in South America and Asia (Carle and Holmgren 2008).

In the early stages of kiln drying, that is, in the presence of liquid water, it is recommended to use low temperatures (below 45 °C) and high RH (above 75 %) (Ciniglio 1998; Andrade 2000). However, these conditions imply long periods of drying, becoming non-economically viable in an industrial scale (Jankowsky and Santos 2005). In contrast, rapid drying is responsible for many wood seasoning defects (Simpson 1991; Denig et al. 2000). Using adequate drying schedules, defects such as cracks, collapse, and warping should be avoided, reducing significantly losses in wood volume and production costs (Martins et al. 2001).

Collapse is one of the most frequent and serious wood drying defects, and *Eucalyptus* are especially susceptible to it (Panshin and de Zeeuw 1980; Vermaas and Bariska 1995; Kauman 2002). Collapse varies significantly among species (Bariska 1992; Vermaas and Bariska 1995). This defect occurs at the beginning of drying, in the presence of liquid water, that is, above the FSP, while normal shrinkage takes place in the hygroscopic range (Panshin and de Zeeuw 1980; Hart 1984; Chafe 1985). Thus, in the case of normal shrinkage, a shrinkage of the cell walls is observed as wood loses bound water, while in the case of collapse, the cell lumens are flattened (Tiemann 1941; Panshin and de Zeeuw 1980; Chafe 1985).

Furthermore, collapse is responsible for severe checking problems in *Eucalyptus* wood, causing important financial loss to wood industry (Blakemore and Northway 2009).

The main purpose of this work was therefore to examine the effect of four desorption rates on dimensional behaviour and the wood–water relationships of never-dried *E. saligna* wood under a wide range of EMC below and above the FSP.

Materials and methods

Samples prepared for this study were obtained from a mature (more than 20 years old) eucalypt tree (*E. saligna*) from a fast-grown plantation located in Itirapina, São Paulo, Brazil (Lat. 22°13′S, 47°50′W). Preliminary tests revealed that *E. saligna* wood is highly prone to collapse.

Samples were prepared from four planks [520 mm (*L*) × 20 mm (*R*) × 20 mm (*T*)] obtained from a single beam [520 mm (*L*) × 110 mm (*R*) × 110 mm (*T*)] stored in green condition (never-dried) at −4 °C and wrapped in polyethylene to prevent moisture loss. The material was without crook, visible decay, with a minimum of knots and grain distortion. The average basic density (BD, oven-dried mass to green volume) of *E. saligna* wood was 515 kg/m^3 [coefficient of variation (CV) of 2.6 %]. According to Brito et al. (2008), the average chemical composition of *E. saligna* is 47 % cellulose, 0.9 % arabinose, 11.5 % mannose, 2.7 % galactose, 6.8 % xylose, 27.1 % lignin, and 4.8 % extractives.

Experiments

Four desorption experiments were conducted with groups of twenty matched cubic samples of 20 × 20 × 20 mm^3 each. All groups of samples were immersed in water and underwent two 24 h cycles of vacuum and atmospheric pressure. Desorption tests were performed from full saturated state until the EMC was reached. One group of twenty samples was destined to the fastest desorption experiment, that is, samples were directly equilibrated from full saturated state to 58 % RH in only one step. Loss of liquid water should occur within this interval of RH. For the three other desorption experiments, intermediate steps were added in order to have four different desorption rates from the saturated state to 58 % RH. Once EMC at 58 % RH was reached, all groups were then equilibrated at 33 % RH and finally 0 % RH (Table 1). After that, adsorption experiments at nearly 100 % RH were carried out for samples of groups 1, 2, and 3 in order to determine the nominal FSP of *E. saligna* wood.

Samples of all groups were conditioned over saturated salt solutions inside tight glass desiccators, except for 0 % RH condition, in which desorption took place over P_2O_5. These small sorption chambers were placed for long periods in vats filled with water, kept at 21 ± 0.01 °C, allowing a precise RH control. A similar procedure has previously been described by Hernández and Bizoň (1994). For each desorption step, all samples were weighed periodically without being removed from the desiccator until the EMC was reached. Except for the 96 % RH condition, in which

Table 1 Steps of the four desorption conditions used for each group of *E. saligna* wood samples

Group	Chemical saturated solutions used for desorption	Nominal RH at 21 °C (%)[a]
1	$NaBr–MgCl_2–P_2O_5$	58–33–0
2	$NaCl–NaBr–MgCl_2–P_2O_5$	76–58–33–0
3	$KCl–NaCl–NaBr–MgCl_2–P_2O_5$	86–76–58–33–0
4	$K_2SO_4–ZnSO_4–KCl–NaCl–NaBr–MgCl_2–P_2O_5$	96–90–86–76–58–33–0

[a] From Almeida et al. (2007)

samples were placed to the next RH condition without attaining EMC, it was assumed that the EMC was reached when the loss in moisture content (MC) was at least <0.01 % per day, considering all twenty samples together.

Once EMC had been reached, samples were individually weighed using an analytical balance to the nearest 0.0001 g in order to determine the EMC of each sample precisely. Immediately, the longitudinal, radial, and tangential dimensions were measured with a micrometer to the nearest 0.001 mm. Samples were then put again inside desiccators to the next desorption step. Dimensional measurements were used to calculate, for each EMC, radial, tangential, and volumetric shrinkage.

Results and discussion

Desorption rates

The loss of MC in all steps of the four desorption conditions as a function of days of experiment is shown in Fig. 1. While samples of the fastest experiment reached EMC at 58 % RH in approximately 90 days, it took more than 500 days for samples submitted to the slowest experiment to reach this condition. However, desorption

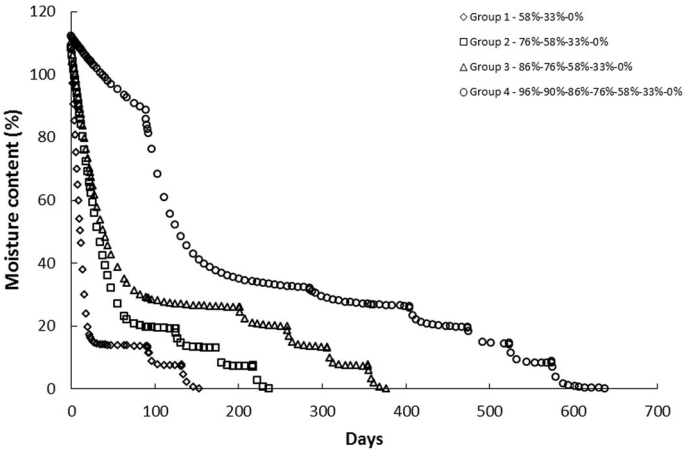

Fig. 1 Loss of MC at each step of the four desorption conditions as a function of time of experiment

Table 2 EMC at the end of each step of desorption for the four experiments

Group	RH (%)				
	90	86	76	58	33
1				13.18[a] (0.04)[b]	7.81 (0.03)
2			18.21 (0.03)	13.26 (0.02)	7.66 (0.02)
3		24.6 (0.1)	18.79 (0.04)	13.43 (0.02)	7.76 (0.02)
4	30.9 (0.3)	24.9 (0.2)	18.61 (0.03)	13.52 (0.02)	7.85 (0.02)

[a] Average of 20 replicates

[b] Standard error of the mean

rates had only a slight effect on EMC, varying from 13.18 % (experiment 1) to 13.52 % (experiment 4) at 58 % RH (Table 2). As reported by other researchers, EMC is a very stable wood physical property if matched samples are equilibrated under a rigorous RH and temperature control (Almeida and Hernández 2006b; Almeida et al. 2007; Passarini et al. 2014, 2015).

In the first step of each desorption condition, i.e. from full saturated state, the desorption rate was higher at low RH, corroborating the observations of Xie et al. (2011). Figure 1 shows that the desorption process is made up of two steps. At the beginning, desorption rate is high, and as it approaches EMC, it is drastically reduced. According to Hill et al. (2010a, b), the sorption behaviour of wood may be described by a model called parallel exponential kinetics (PEK). This model is composed of two exponential terms which represent the fast and slow processes having characteristic times and moisture contents associated with them (Hill et al. 2010a, b, 2012). As shown in Fig. 1, greater amounts of moisture were lost during the fastest process.

Molecular rearrangements within the cell wall are related to the reduction of sorption rate (Hill et al. 2010a). It could then be hypothesised that these rearrangements might be more intense at the end of the desorption step. From T_2 times obtained by NMR analyses of water in wood, bound water is more tightly attached to wood at lower MC (Almeida et al. 2007; Thygesen and Elder 2008; Cox et al. 2010; Elder and Houtman 2013; Zhang et al. 2013; Passarini et al. 2014), which could hinder water loss and reduce desorption rate.

Dimensional changes and wood–water relationships

The partial and total shrinkages of *E. saligna* wood samples submitted to four desorption rates are presented in Table 3. Total shrinkage increased as desorption rate decreased. Partial shrinkage, obtained from saturated state to 58 % RH, showed the same behaviour. However, shrinkage from 58 % RH to 0 % RH (6.4 % for groups 1, 2, and 3, and 6.6 % for group 4, respectively) was not affected by the desorption rates. The difference in shrinkage among the four desorption rates was therefore produced before reaching this RH condition (58 % RH). According to Passarini et al. (2014), all loss of liquid water of *E. saligna* wood could have occurred above 58 % RH. In fact, Fig. 2 shows that shrinkage values obtained at

Table 3 Partial shrinkage, total shrinkage, and estimated collapse for the four desorption conditions

Group	Shrinkage from full saturated state to 58 % RH (%)			Total shrinkage (%)			Estimated collapse (%)[c]	
	R	*T*	*V*	*R*	*T*	*V*	*R*	*T*
1	3.77[a] (0.05)[b]	8.2 (0.1)	11.6 (0.1)	6.93 (0.06)	11.9 (0.1)	18.0 (0.1)	0.6	0.9
2	3.97 (0.04)	8.5 (0.2)	12.1 (0.2)	7.16 (0.04)	12.2 (0.2)	18.5 (0.1)	0.9	1.2
3	3.99 (0.05)	8.7 (0.1)	12.4 (0.1)	7.18 (0.06)	12.5 (0.1)	18.8 (0.1)	0.9	1.5
4	4.17 (0.05)	9.0 (0.1)	12.8 (0.2)	7.39 (0.06)	12.9 (0.1)	19.4 (0.1)	1.1	1.9

R radial direction, *T* tangential direction, *V* volumetric shrinkage

[a] Average of 20 values

[b] Standard error of the mean

[c] Estimated from Almeida et al. (2009)

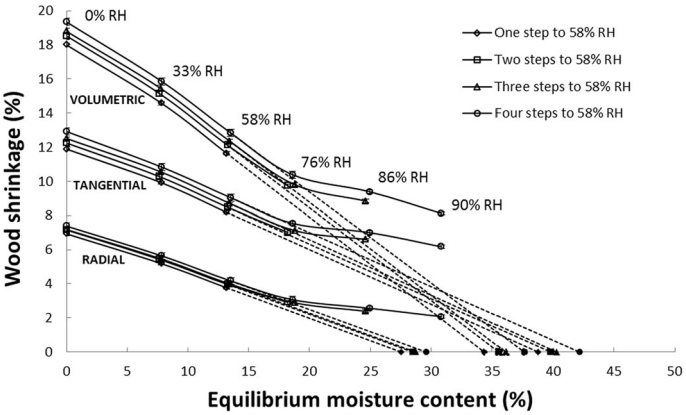

Fig. 2 Radial, tangential, and volumetric shrinkages of *E. saligna* wood as a function of EMC at 21 °C. The *symbols* on the *x*-axis represent the FSP estimated by the shrinkage intersection point method (standard errors are shown only when it exceeds the *symbol size*). The 96 % RH step is not included in this graphic because equilibrium was not reached

58 % RH are located in the straight linear part of the relationship between shrinkage and EMC. This figure also indicates that above nearly 76 % RH the shrinkage–EMC curves are shifted upwards in relation to their extended straight linear portion. This demonstrates that differences in shrinkage among the four desorption rates were established in the presence of liquid water.

Shrinkage is responsible for large stresses in wood as a result of wood heterogeneity and anisotropy even under no external loads (Hsu and Tang 1974). Considering these stresses, the long periods involved and the very strict temperature and RH controls during each step of the desorption experiments, it could be hypothesised that time-dependent creep (or viscoelastic creep) might explain these findings. In this case, faster desorption rates could create higher tension strains at the outer layer of samples, especially at high RH, tensions which are responsible for lower shrinkage in the core layer. Thus, overall shrinkage of samples would be

lower. If this hypothesis is true, the time-dependent creep could be responsible for a volumetric shrinkage 10 % higher for group 4 in relation to group 1.

Eucalyptus wood is highly prone to collapse (Panshin and de Zeeuw 1980; Chafe 1985; Vermaas and Bariska 1995; Kauman 2002). As explained before, collapse is a form of shrinkage which occurs during drying in most species of wood, reducing greatly the size of lumens (Kuo and Arganbright 1978; Chafe 1985; Blakemore and Northway 2009). It takes place in the early stages of drying in the presence of liquid water that is above the FSP, while the normal shrinkage occurs in the hygroscopic domain (Panshin and de Zeeuw 1980; Hart 1984; Chafe 1985). High values of radial and tangential shrinkage might be indicative of collapse (Santos 2002).

Almeida et al. (2009) carried out radial and tangential shrinkage measurements in 1-mm-thick samples of *E. saligna* wood from a Brazilian plantation. These thin sections are expected to be collapse-free and thus represent only shrinkage of cell walls (Kelsey 1956; Chafe and Ilic 1992). Total radial and tangential shrinkages from Almeida et al. (2009) were lower than those observed in the present work. Collapse may be estimated as the difference between total shrinkage and shrinkage from collapse-free samples (Chafe and Ilic 1992). From this, collapse was estimated taking the values of Almeida et al. (2009) and those obtained in the present work (Table 3). Collapse in radial direction varied from 0.6 % (group 1, fastest desorption rate) to 1.1 % (group 4, slowest desorption rate). In tangential direction, collapse was higher and was estimated to vary from 0.9 % (group 1) to 1.5 % (group 4, Table 3). This anisotropy in *Eucalyptus* collapse has already been observed elsewhere (Bariska 1992). The movement of liquid water from heartwood fibres to the rays in the tangential direction (Bariska 1992) and the mechanical contribution of rays in the radial direction (Wilkes and Wilkins 1987) might explain this behaviour. In addition, the largest collapse in the tangential direction might also be an indicator of the lower mechanical strength of wood in the tangential direction (Bariska 1992; Demanet and Morlier 2000).

Radial, tangential, and volumetric shrinkages as a function of EMC are presented in Fig. 2. In all cases, these curves exhibit a straight linear behaviour only between 58 and 33 % RH (approximatively between 13 and 8 % EMC). The linear portions remained parallel for the four desorption rates, revealing again that desorption rates affected shrinkage intensity without changing its behaviour in these portions of the curves. Almeida et al. (2009) obtained similar results studying the effect of heat treatment on shrinkage behaviour of three *Eucalyptus* woods. This indicates that the distances among the four shrinkage–EMC curves were generated at the beginning of desorption when collapse and loss of liquid water occur. Shrinkage and collapse could be more intense if desorption experiments were carried out at higher temperatures. Thus, judicious drying schedules should be employed in order to add quality and value to *E. saligna* wood.

According to Kelsey (1956), the MC at which the extended straight linear portion of the shrinkage–MC curve intersects the line of zero shrinkage is defined as the shrinkage intersection point (SIP). This point is one of several methods to determine the FSP (Almeida et al. 2009). In the present study, the intersection point for radial, tangential, and volumetric shrinkages was determined from the region between 33 and 58 % of the shrinkage–EMC curves (Fig. 2). For all directions, the FSP

Table 4 Fibre saturation point determined by the shrinkage intersection point method for the four desorption conditions

Group	Shrinkage intersection point (SIP) (%)			FSP (%)[b]
	R	*T*	*V*	
1	27.5[a]	38.8	34.4	28.8
2	28.5	39.8	35.6	29.2
3	28.7	40.3	36.1	28.8
4	29.6	42.2	37.6	–

R radial direction, *T* tangential direction, *V* volumetric shrinkage

[a] Average of 20 replicates

[b] Determined in adsorption under 100 % RH

increased as the desorption rate decreased (number of desorption steps increased), especially for the tangential direction (Table 4). The presence of collapse shifted upwards all shrinkage–EMC curves and these remained parallel, making determination of FSP by the SIP not feasible for collapse-prone wood species. The actual FSP of this species, determined in adsorption under nearly 100 % RH, was about 29 % MC (Table 4).

Considering the FSP for *E. saligna* wood as 29 % MC, Fig. 2 shows that shrinkage in all directions and, consequently, in volume, sets off well above FSP (Hernández and Bizoň 1994; Hernández and Pontin 2006; Almeida and Hernández 2006a, b). These researchers also reported the phenomenon of hysteresis at saturation on shrinkage at high EMC, which affected the wood moisture sorption above 65 % RH (Stamm 1971; Hernández 1983). It implies that, during desorption, loss of bound water takes place before cellular cavities are emptied of liquid water. The range of MC corresponding to this region will depend on the size distribution of wood capillaries and, as a result, will vary among wood species (Almeida and Hernández 2006a, b, 2007, Hernández and Pontin 2006).

Slight amounts of liquid water entrapped in axial parenchyma of small samples of *E. saligna* wood at 90 % RH (25.8 % EMC) were disclosed by high-resolution magnetic resonance images (Passarini et al. 2015). However, at 76 % RH, this water had been completely drained (Passarini et al. 2015). In the present study, liquid water seems to be entrapped in samples as low as about 76 % RH, that is, the RH at which shrinkage–EMC curves begin to depict a straight linear behaviour as wood dries. This might be explained by the larger size of samples (20 mm cubic samples), hampering the drainage of liquid water in relation to those used by Passarini et al. (2015) (2-cm-long cylinders by 3.6 mm in diameter).

Conclusion

The effects of four desorption experiments carried out under isothermal conditions on the shrinkage behaviour and on the wood–water relationships of never-dried *E. saligna* wood were evaluated. A large range of MC below and above the FSP was

studied in order to better understand the loss of both bound and liquid waters and their influence on wood physical properties. The main conclusions which may be drawn from this work are:

1. Radial, tangential, and volumetric shrinkages were higher when wood was submitted to slower desorption rates. Viscoelastic creep might be involved in these findings.
2. Estimated collapse of cell lumens varied between 0.6 and 1.1 % in radial direction and between 0.9 and 1.9 % in tangential direction. Milder desorption rates implied a higher collapse in both directions.
3. Under the hygroscopic range between 0 and 58 % RH, the slope of shrinkage–EMC curves was not affected by the desorption rate.
4. The FSP, established by the SIP method, increased as the desorption rate decreased, especially in the tangential direction. The values obtained were excessively high, revealing that this method is not convenient for a collapse-prone wood like *E. saligna*.
5. At about 76 % RH (20 % EMC) or higher, *E. saligna* wood presented entrapped liquid water, confirming the existence of a region in the hygroscopic range in which the loss of bound water takes place before all liquid water has been drained.

Acknowledgments The authors are grateful to Professor Yves Fortin for valuable suggestions in the analysis of results of this work. This research was supported by the Natural Sciences and Engineering Research Council of Canada.

References

Almeida G, Hernández RE (2006a) Changes in physical properties of tropical and temperate hardwoods below and above the fiber saturation point. Wood Sci Technol 40:599–613

Almeida G, Hernández RE (2006b) Changes in physical properties of yellow birch below and above the fiber saturation point. Wood Fiber Sci 38:74–83

Almeida G, Hernández RE (2007) Dimensional changes of beech wood resulting from three different re-wetting treatments. Holz Roh Werkst 65:193–196

Almeida G, Gagné S, Hernández RE (2007) A NMR study of water distribution in hardwoods at several equilibrium moisture contents. Wood Sci Technol 41:293–307

Almeida G, Brito JO, Perré P (2009) Changes in wood-water relationship due to heat treatment assessed on micro-samples of three Eucalyptus species. Holzforschung 63:80–88

Andrade A (2000) Indicação de programas para a secagem convencional de madeiras (Suggestion of kiln schedules to conventional drying of lumber). M.Sc. Thesis. Universidade de São Paulo, Piracicaba, Brazil (**in Portuguese**)

Bariska M (1992) Collapse phenomena in eucalypts. Wood Sci Technol 26:165–179

Blakemore P, Northway R (2009) Review of, and recommendations for, research into preventing or ameliorating drying related internal and surface checking in commercially important hardwood species in South-eastern Australia. FWPA Project PNB047-0809. http://www.fwpa.com.au/images/processing/PNB047-0809_Research_Report_Surface_Internal_0.pdf. Accessed 12 June 2014

Brito JO, Silva FG, Leão MM, Almeida G (2008) Chemical composition changes in eucalyptus and pinus woods submitted to heat treatment. Bioresour Technol 99:8545–8548

Brown HP, Panshin AJ, Forsaith CC (1952) Textbook of wood technology. The physical, mechanical, and chemical properties of the commercial wood of the United States, vol II. McGraw-Hill, New York

Carle J, Holmgren P (2008) Wood from planted forests, a global outlook 2005–2030. Forest Prod J 58:6–18

Chafe SC (1985) The distribution and interrelationship of collapse, volumetric shrinkage, moisture-content and density in trees of *Eucalyptus regnans* F Muell. Wood Sci Technol 19:329–345

Chafe SC, Ilic J (1992) Shrinkage and collapse of thin sections and blocks of Tasmanian mountain ash regrowth. Part 3: collapse. Wood Sci Technol 26:343–351

Ciniglio G (1998) Avaliação da secagem de madeira serrada de *E. grandis* e *E. urophylla*. (Drying assessment of *E. grandis* and *E.urophylla* lumber). M.Sc. Thesis. Universidade de São Paulo, Piracicaba, Brazil (**in Portuguese**)

Cox J, McDonald PJ, Gardiner PA (2010) A study of water exchange in wood by means of 2D NMR relaxation correlation and exchange. Holzforschung 64:259–266

Demanet A, Morlier P (2000) Mécanismes du collapse du chêne séché sous vide en vapeur d'eau surchauffée (Collapse mechanisms of oak wood dried under vacuum with superheated steam). Ann For Sci 57:165–179 **(in French)**

Denig J, Wengert EM, Simpson WT (2000) Drying hardwood lumber. Gen Tech Rep FPL-GTR-118. Department of Agriculture, Forest Service, Forest Products Laboratory, Madison

Elder T, Houtman C (2013) Time-domain NMR study of the drying of hemicellulose extracted aspen (*Populus tremuloides* Michx.). Holzforschung 67:405–411

FAO (1981) El eucalipto en la repoblación forestall (Eucalypts for planting). Colección FAO: estudios de silvicultura y productos forestales 11. FAO, Rome (**in Spanish**)

Forest Products Laboratory (FPL) (2010) Wood handbook—wood as an engineering material. General technical report FPL–GTR–190. Department of Agriculture, Forest Service, Forest Products Laboratory, Madison

Hart CA (1984) Relative humidity, EMC, and collapse shrinkage in wood. Forest Prod J. 34(11/12):45–54

Hernández RE (1983) Relations entre l'état de sorption et la résistance du bois d'érable à sucre en traction tangentielle (Influence of moisture sorption on the strength of sugar maple wood in tangential tension). M.Sc. Thesis. Département d'exploitation et utilisation des bois, Université Laval, Québec (**in French**)

Hernández RE, Bizoň M (1994) Changes in shrinkage and tangential compression strength of sugar maple below and above the fiber saturation point. Wood Fiber Sci 26:360–369

Hernández RE, Pontin M (2006) Shrinkage of three tropical hardwoods below and above the fiber saturation point. Wood Fiber Sci 38:474–483

Hill CAS, Norton A, Newman G (2010a) Analysis of the water vapour sorption behaviour of Sitka spruce [*Picea sitchensis* (Bongard) Carr.] based on the parallel exponential kinetics model. Holzforschung 64:469–473

Hill CAS, Norton A, Newman G (2010b) The water vapour sorption properties of Sitka spruce determined using a dynamic vapour sorption apparatus. Wood Sci Technol 44:497–514

Hill CAS, Keating BA, Jalaludin Z, Mahrdt E (2012) A rheological description of the water vapour sorption kinetics behaviour of wood invoking a model using a canonical assembly of Kelvin–Voigt elements and a possible link with sorption hysteresis. Holzforschung 66:35–47

Hsu NN, Tang RC (1974) Internal stresses in wood logs due to anisotropic shrinkage. Wood Sci 7:43–51

Jankowsky IP, Santos GRV (2005) Drying behaviour and permeability of *Eucalyptus grandis* lumber. Maderas Cienc Tecnol 7(1):17–21

Jankowsky IP, Santos GRV, Andrade A (2008) Secagem da madeira serrada de eucalipto (Drying behavior of eucalyptus lumber). Revista da Madeira 19:64–72 **(in Portuguese)**

Kauman WG (2002) Contribution to the theory of cell collapse in wood: investigations with eucalyptus regnans. Maderas Ciencia y tecnología 4:77–99

Kelsey KE (1956) The shrinkage intersection point—its significance and the method of its determination. For Prod J 6:411–416

Kuo ML, Arganbright DG (1978) SEM observation of collapse in wood. IAWA Bull 2–3:40–46

Martins VA, Gouveia FN, Martinez S (2001) Secagem convencional de madeira de eucalipto parte I: *Eucalyptus cloeziana* F. Muell, *E. grandis* Hil Ex Maiden e *E. pilularis* Sm (Conventional drying of eucalypts part I: *Eucalyptus cloeziana* F. Muell, *E. grandis* Hil Ex Maiden and *E. pilularis* Sm. Brasil Florestal 70:42–47 **(in Portuguese)**

Panshin AJ, de Zeeuw C (1980) Textbook of wood technology. Michigan State University, New York

Passarini L, Malveau C, Hernández RE (2014) Water state study of wood structure of four hardwoods below fiber saturation point with NMR technique. Wood Fiber Sci 46:480–488

Passarini L, Malveau C, Hernández RE (2015) Distribution of the equilibrium moisture content in four hardwoods below fiber saturation point with magnetic resonance microimaging. Wood Sci Technol 49(6):1251–1268

Santos JA (2002) Recovering dimension and form in collapse distorted boards. In: Proceedings of 4th Cost E15 Workshop. Santiago de Compostela, Spain

Shmulsky R, Jones P (2011) Forest products and wood science, an introduction. Blackwell, Ames

Siau JF (1984) Transport processes in wood. Springer, Berlin

Simpson WT (1991) Dry kiln operator's manual. USDA, FPL No. 188, Madison, Wisconsin

Skaar C (1988) Wood-water relations. Springer, Berlin

Stamm AJ (1971) Review of nine methods for determining the fiber saturation point of wood and wood products. Wood Sci 4:114–128

Thygesen LG, Elder T (2008) Moisture in untreated, acetylated, and furfurylated Norway spruce studied during drying using time domain NMR. Wood Fiber Sci 40:309–320

Tiemann HD (1906) Effect of moisture upon the strength and stiffness of wood. U.S.D.A. Forest Service, Bulletin 70

Tiemann HD (1941) Collapse in wood as shown by the microscope. J Forest 39:271–283

Turnbull JW (1999) Eucalypt plantations. New Forest 17:37–52

Vermaas HF (1995) Drying eucalyptus for quality: material characteristics, pre-drying treatments, drying methods, schedules and optimisation of drying quality. S Afr For J 174:41–49

Vermaas HF, Bariska M (1995) Collapse during low temperature drying of *Eucalyptus grandis* W Hill and *Pinus sylvestris* L. Holzforsch Holzverw 47:35–40

Wilkes J, Wilkins AP (1987) Anatomy of collapse in eucalyptus species. IAWA Bull 8:291–295

Xie Y, Hill CAS, Xiao Z, Mai C, Militz H (2011) Dynamic water vapour sorption properties of wood treated with glutaraldehyde. Wood Sci Technol 45:49–61

Zhang M, Wang X, Gazo R (2013) Water states in yellow poplar during drying studied by time-domain nuclear magnetic resonance. Wood Fiber Sci 45:423–428